

ARTICLE

Photophysical Property of Photoactive Molecules with Multibranched Push-Pull Structures[†]

Ying-ying Wang, Xiao-nan Ma, Silviije Vdović, Lin-yin Yan, Xue-fei Wang, Qian-jin Guo, An-dong Xia*

The State Key Laboratory of Molecular Reaction Dynamics, Beijing National Laboratory for Molecular Sciences, Institute of Chemistry, Chinese Academy of Sciences, Beijing 100190, China

(Dated: Received on August 17, 2011; Accepted on September 7, 2011)

The structure-property characteristics of a series of newly synthesized intramolecular charge-transfer (ICT) compounds, single-branch monomer with triphenylmethane as electron donor and 2,1,3-benzothiadiazole as acceptor, the corresponding two-branch dimer and three-branch trimer, have been investigated by means of steady-state and femtosecond time-resolved stimulated emission fluorescence depletion (FS TR-SEP FD) techniques in different polar solvents. The TD-DFT calculations are further performed to explain the observed ICT properties. The interpretation of the experimental results is based on the comparative studies of the series of compounds which have increased amount of identical branch moiety. The similarity of the absorption and fluorescence spectra as well as strong solvent-dependence of the spectral properties for the three compounds reveal that the excited state of the dimer and trimer are nearly the same with that of the monomer, which may localize on one branch. It is found that polar excited state emerged through multidimensional intramolecular charge transfer from the donating moiety to the acceptor upon excitation, and quickly relaxed to one branch before emission. Even so, the red-shift in the absorption and emission spectra and decreased fluorescence radiative lifetime with respect to their monomer counterpart still suggest some extent delocalization of excited state in the dimer and trimer upon excitation. The similar behavior of their excited ICT state is demonstrated by FS TR-SEP FD measurements, and shows that the trimer has the largest charge-separate extent in all studied three samples. Finally, steady-state excitation anisotropy measurements has further been carried out to estimate the nature of the optical excitation and the mechanism of energy redistribution among the branches, where no plateau through the ICT band suggests the intramolecular excitation transfer process between the branches in dimer and trimer.

Key words: Branched intramolecular charge transfer molecule, Fluorescence decay, Femtosecond time-resolved stimulated emission fluorescence depletion, Steady-state excitation anisotropy

I. INTRODUCTION

Organic molecules with intramolecular charge transfer (ICT) properties have been studied extensively on both photochemical and photophysical properties, for their great potential applications in a large number of areas, such as organic solar cells [1–3] and nonlinear optics in the last decade [4–6]. Recently, large molecular aggregates, such as dendrimers and multi-branched organic molecules, have received wide interest, because they show enhanced optical properties especially in two-photon absorption (TPA) properties, faster

charge transfer processes and conversion efficiency with respect to their monomer counterparts. Significant research has been carried out in synthesizing novel multiple dimensionality branched chromophores with different donor-acceptor moieties to improve their optical properties. Thus, further work on explaining the structure-to-property relationships, both theoretically and experimentally, are more important in order to support the design and synthesis of novel materials with better optical properties.

The fundamental challenge in such branched ICT molecular photophysics is to understand the photoexcitation energy transfer between different arms and excitation energy location or the degree of the delocalization. If the branching center disrupts the conjugation due to the molecular nuclear motion or interactions with the surroundings, excitation energy would stabilize localized on one arm or some parts, and there is almost

[†]Part of the special issue for “the Chinese Chemical Society’s 12th National Chemical Dynamics Symposium”.

*Author to whom correspondence should be addressed. E-mail: andong@iccas.ac.cn

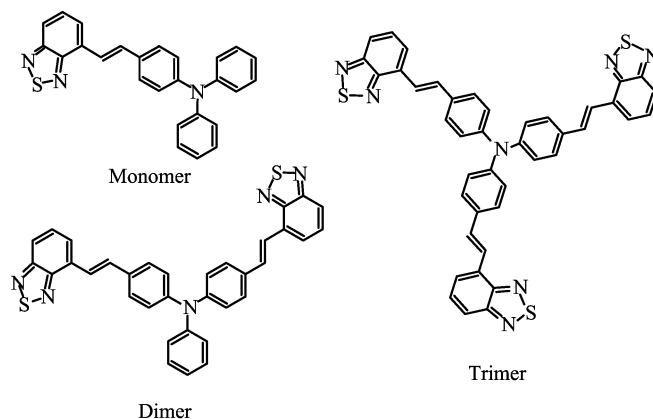
no coupling or weak interaction between branches, such as in phenyl-acetylene dendrimers [7, 8] and a series of triphenylamine chromophores [9, 10]. The excited-state dynamic and the mechanisms of excitation energy transfer are still challenging themes to be explored. Goodson and co-workers had used the femtosecond time-resolved fluorescence anisotropy measurements and transient absorption techniques to reveal the complicate intrachromophore interactions in PRL series dyes [6, 11, 12]. Incoherent or hopping dynamics and coherent interactions [8, 10, 11] can be involved depending on the different donor or acceptor, geometrical structure and symmetry. Taking into account of the intrinsic complexity of such molecules, we pursue to perform systematic investigation of compounds with exactly identical ICT chromophores but an increased number of branches through steady state and transient optical experiment, in order to get the information about fundamental mechanisms of energy redistribution as well as the localization or delocalization of the excited state in such a series of compounds.

In this work, we have carried out steady state and transient optical experiments on three newly synthesized ICT compounds, which share a strong electron donor triphenylmethane in the center, with 2,1,3-benzothiadiazole as acceptor in the end of each branch, linked by ethylene bond. Scheme 1 shows the molecular structures of monomer, dimer, and trimer. The results of steady-state spectral experiments show that the excited ICT state of the dimer and trimer exhibit similar spectral behaviors to that of monomer in different solvents, which indicate that the excited state quickly relaxes to one branch after the delocalized excitation. Besides, some different spectral properties are still observed with some extent delocalization of the excited state in the branched dimer and trimer. This phenomenon has not been widely observed in previous literatures due to different chromophore structure and solvent used in experiments. We further use home-made femtosecond time-resolved stimulated emission fluorescence depletion to determine ultrafast charge transfer dynamics. We find that the trimer has the largest charge-separate extent, similar to previous research reported by Goodson in their femtosecond transient absorption investigation [12], suggesting that it may be a common feature for molecules of such a structure. The details may help to understand the structure-property relationship of large ICT system in the case of the solvents with different polarity, which may make the optical behavior more complex in practical cases.

II. MATERIALS AND METHODS

A. Materials

The monomer, dimer, and trimer were synthesized by palladium-catalyzed Heck reaction using triphenyl-



Scheme 1 Molecular structures of monomer, dimer, and trimer.

amine as the π -electron donor together with benzothiadiazole as the π -electron acceptor, which connected with the donor. Details on the synthesis and characterization had been reported elsewhere [3]. The chemical structures and purities were identified by NMR and MALDI-TOF-MS. All the aprotic solvents including cyclohexane, toluene, chloroform, tetrahydrofuran, acetonitrile and acetone used in this work were of A.R. grade or higher, and used as received from the Beijing Chemical Plant without further purification. Fluorescein was purchased from Sigma-Aldrich.

B. Absorption and fluorescence measurements

UV-Vis absorption spectra were recorded with a Model U3010 (HITACHI) spectrophotometer. Corrected fluorescence and excitation spectra were obtained with a Hitachi F-4600 fluorescence spectrometer using a Xe lamp as the excitation source. The fluorescence quantum yields were determined using fluorescein solved in 0.1 mol/L sodium hydroxide at 25 ± 5 °C as a reference ($\phi_F=0.90$) [13]. The fluorescence lifetimes of the three compounds were collected by means of a time-correlated single photon counting (TCSPC) apparatus with 200 ps time resolution using a scatter solution to obtain the instrument response function (IRF). For TCSPC measurement, an excitation wavelength of 450 nm was used to excite the samples.

C. Excitation anisotropy measurements

Excitation anisotropy spectra were measured with a fluorescence spectrophotometer (F4600, Hitachi) by passing the excitation and emission light through a Glan-Thompson polarizer, and determined according to the

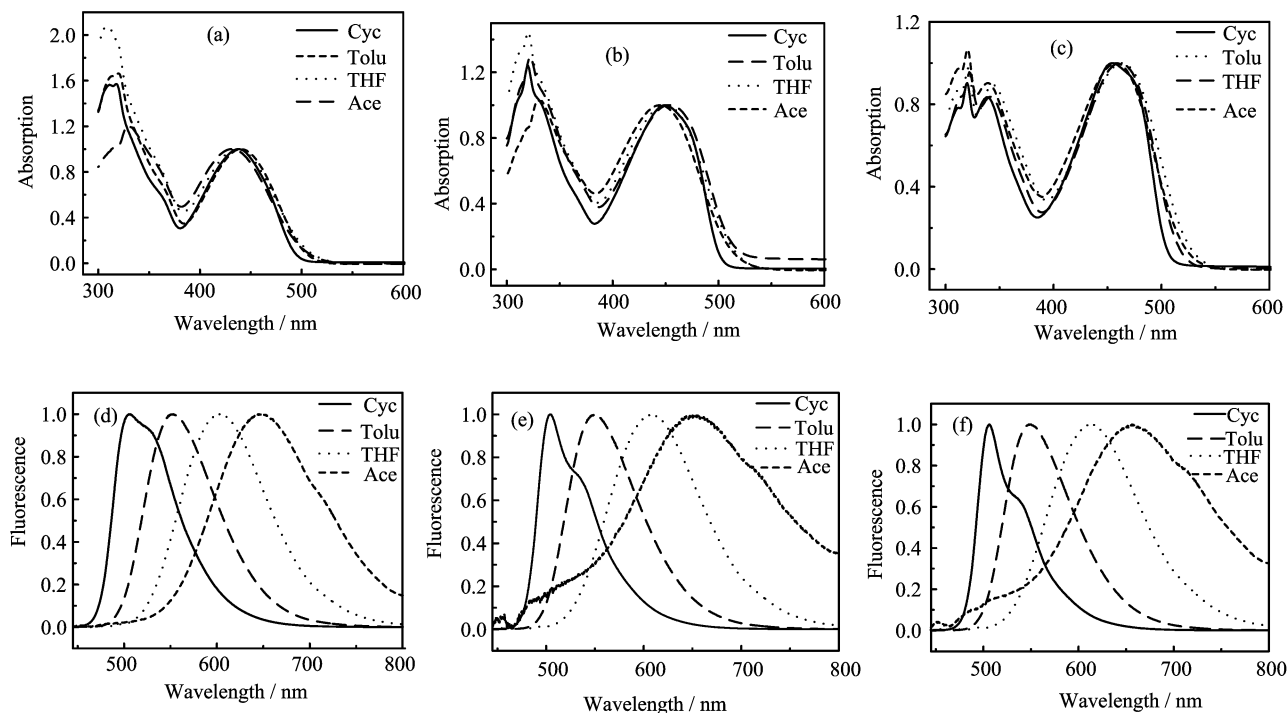


FIG. 1 Normalized steady-state absorption of (a) monomer, (b) dimer, and (c) trimer and emission spectra of (d) monomer, (e) dimer, and (f) trimer in different solvents of cyclohexane (Cyc), toluene (Tolu), tetrahydrofuran (THF), and acetone (Ace).

following function:

$$r = \frac{I_{//} - GI_{\perp}}{I_{//} + 2GI_{\perp}} \quad (1)$$

where $I_{//}$ and I_{\perp} are the observed intensities parallel and perpendicular to the electric vector of the excitation light, respectively, and G is instrumental factor given by $G=I_{\perp}/I_{//}$, when the excitation is vertically polarized.

D. Femtosecond fluorescence depletion measurements

Fluorescence depletion was conducted using a home-made femtosecond time-resolved stimulated emission depletion setup (TR-STED) as that shown in our previous publication [14–17]. The principle involved in the TR-STED experiment was described elsewhere [14–19]. In brief, a femtosecond laser pulse was used as pump beams to excite the chromophores from the electronic ground-state S_0 to a Franck-Condon level S_1^* . The second femtosecond probe at the magic angle (54.7°) with respect to pump polarization pulse with a delay time was applied to the excited molecules to induce stimulated emission from relaxed electronic state S_1 to the vibrationally excited ground level S_0^* . The IRF was determined based on the nondegenerated two-photon excited fluorescence method, from which the IRF down to 200 fs was achieved. All the temporal evolution profiles were deconvoluted from the IRF and fitted to

single (double) exponential function of time according to iterative reconvolution by FluoFit software based on the Levenberg-Marquardt and Simplex algorithms (Version3.1, PicoQuant, Germany). The quality of the fits was judged by weighted residuals and reduced χ^2 values. All experiments presented in this work were performed at room temperature.

III. RESULTS AND DISCUSSION

A. Optical absorption and steady-state fluorescence measurements

Figure 1 shows normalized steady-state absorption and emission spectra of monomer, dimer, and trimer in a series of aprotic solvents with similar refractive index and different polarity. The spectra of these three samples in different solvents present the similar spectral properties. It is observed that the absorption spectra consist of two main broad bands ranging from 300 nm to 540 nm. The band in blue side is mainly attributed to the π - π^* transition, whereas that in red side results from the ICT as many other researchers reported [15, 20–22]. Fluorescence emission obviously red-shift with the increase of solvent polarities relative to the absorption spectra, suggesting energy reorganization before emission, which is typical of the fluorescence from the relaxed ICT states. All three molecules show marked positive emission solvatochromism, whereas the max-

TABLE I Solvent parameters, Stokes shift, and fluorescence quantum yield of monomer, dimer, and trimer.

Solvent	Parameter ^a				Stokes shift			Quantum yield		
	ϵ	n	Δf	F^b	Monomer	Dimer	Trimer	Monomer	Dimer	Trimer
Cyc	2	1.424	-0.0033	0	3044.72	2422.57	2330.79	0.50	0.65	0.67
Toluene	2.4	1.494	0.0159	0.02	4650.62	3844.61	3477.04	0.54	0.53	0.54
Ms(1) ^c	2.882	1.483	0.0561	0.09	5437.33	4760.39	4343.98	0.39	0.36	0.37
Ms(2) ^c	3.605	1.468	0.0998	0.28	6031.26	5296.42	5077.76	0.26	0.26	0.27
Chlo	4.81	1.443	0.1493	0.29	6521.70	5934.92	5701.96	0.18	0.16	0.12
THF	7.6	1.405	0.2100	0.44	6332.48	5764.03	5542.11	0.29	0.25	0.2
Ms(3) ^c	13.3	1.393	0.2530	0.56	7023.32	6428.23	6241.09	0.16	0.06	0.04
Acetone	20.6	1.356	0.2850	0.65	7707.59	7218.70	6399.69	0.065	0.005	0.005

^a Parameters are taken from Ref.[27]. ϵ is the dielectric constant and n is the refractive index of the solvent. Δf is the solvent polarity function.

^b Reaction field factor.

^c MS, mixed solvent of toluene and chloroform. For MS(1) and MS(2) with volume ratio about 8:2. and 5:5, respectively. Mixed solvents of THF and acetonitrile for MS(3) with volume ratios about 8:2. The corresponding ϵ mix and n mix values are obtained by the expressions $\epsilon_{\text{mix}}=f_a\epsilon_a+f_b\epsilon_b$ and $n_{\text{mix}}^2=f_a n_a^2+f_b n_b^2$, respectively [27].

ima and shape of the absorption spectra almost have no change with solvent polarity. The fluorescence emission maxima significantly shifts to low energy with the increased solvent polarity while the vibrational structure appeared in the nonpolar cyclohexane and disappeared in more polar solvents Tolu, THF, and Ace, becoming a broad structureless band [23]. A successive decrease in the fluorescence quantum yield is also found in more polar solvents. Such behavior is consistent with the stabilization of highly polar emitting excited state in polar solvents. The results in different solvents are summarized in Table I.

Comparing the steady-state spectra of the three compounds in toluene, it can be seen that absorption maxima of the higher-energy bands remains essentially the same, but the lower-energy ICT absorption band shifts to longer wavelengths as the number of branches per molecule is increased. This means some interactions exist between the branches in the molecule, which may result in charge redistribution and extended delocalization, where the lone pair electron on the central nitrogen atom plays important role on delocalization among the branches [24]. However, unlike the bathochromic shift in the absorption spectra from monomer, dimer, and trimer, we observed nearly identical but only a small red shift fluorescence spectrum in toluene for these samples, which is attributed to the similar emission nature relative to the monomer. The emission from dimer and trimer also locate on one branch after excitation [23]. The localized emission behavior is probably due to the use of the amino group as the center connecting unit, where the mesomeric effect breaks down the conjugation. In particular, symmetry breaking upon excitation in molecule dimer with 2-fold or trimer with 3-fold symmetries, leading to a polar singlet excited state, has been proved theoretically to be a general appearance in multibranch structures [15, 22]. Furthermore, the red

shift of the fluorescence spectra in more polar solvent THF is also seen in the dimer and trimer, suggesting that the charge-transfer degree in trimer is larger than that in the dimer and the monomer.

B. Quantum chemical calculations

We performed the density functional theory (DFT) methods as implemented in the Gaussian 03 software package. Solvation effects were neglected during calculation. The ground state geometries of the three molecules are fully optimized under B3LYP/6-311G(d,p) level [15, 22]. As chromophores with the triphenylamine moiety adopt a propeller-shaped structure, the phenyl rings are twisted with respect to the trigonal planar nitrogen (dihedral angle smaller than 1°), twist angle is between 34° and 46° . The conjugated stilbenyl branches are found to be almost planar. Overall, all branches in dimer and trimer have ground-state geometries similar to the geometry of the monomer, twist angles are slightly less than that in monomer for the same substituents on each branch. This implies that branched compounds have higher symmetries (*e.g.*, C_3 for trimer). Unfortunately, we don't have the capability to perform excited-state geometries optimization. According to calculations performed on similar systems [10], we suppose to apply their conclusions to our systems, that the monomer becomes planar upon excitation, which is a general phenomenon observed in many extended molecular systems such as conjugated polymers [25, 26]. It is found that only one branch in dimer and trimer gets planar, the remaining parts are still in ground structure, suggesting the similar excited state character with monomer.

DFT calculation indicates the pronounced multidimensional intramolecular charge transfer characters oc-

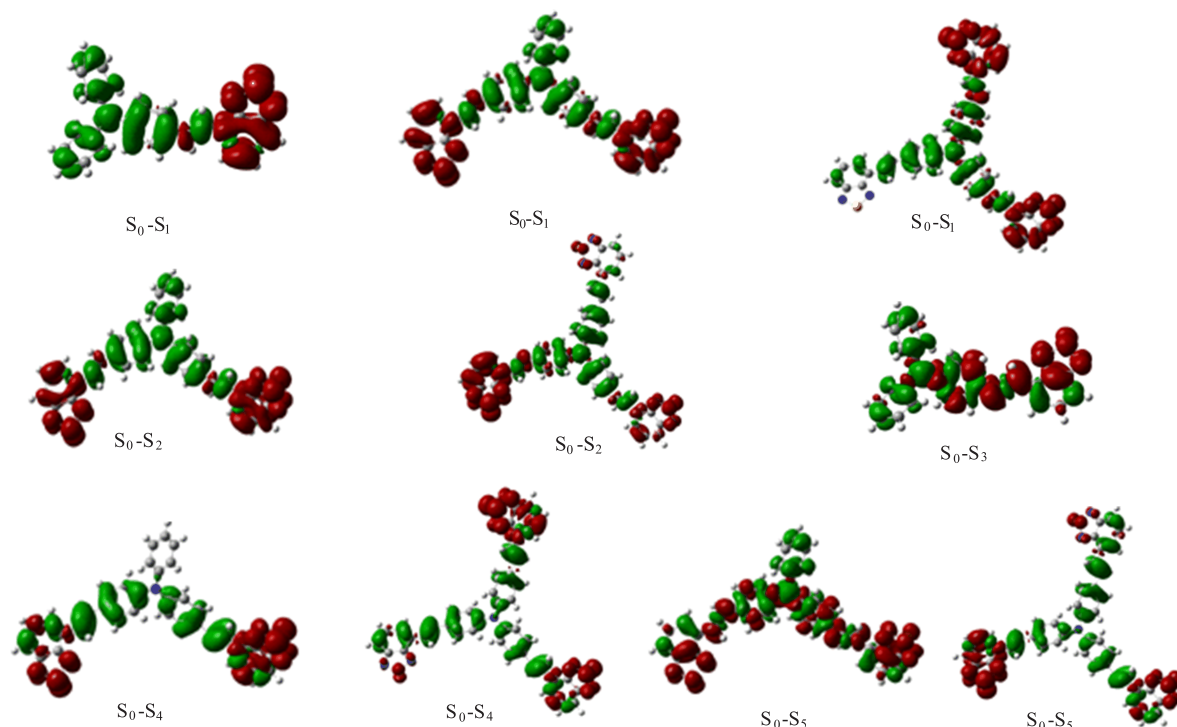


FIG. 2 The charge density difference (CCD) of the first few states with oscillator strength larger than 0.1. The red color represents the electron density gain, and the green loss. For the interpretation of the color in this figure legend, the reader can refer to the web version of this article.

curred within the chromophores upon excitation. Indeed, the charge density difference (CCD) of the first excited state(s) shown in Fig.2 reveals pronounced electronic density shifts from the triphenylamine moiety to the conjugated branch in all three chromophores, and shows typical ICT characters in all three molecules.

C. Solvation effect

As mentioned above, the absorption spectra of all the compounds are less dependent on the polarity of the solvents, while the fluorescence spectra show strongly solvent-dependent red-shift with the increased polarity. To elaborate the solvent-dependent properties, we use Lippert-Mataga relationship for further discussion. The Lippert-Mataga relationship is usually used to measure the solvent-dependent shift of the emission maximum and the change of the dipole moment between the excited-state and ground-state dipole moments upon excitation only for nonspecific interaction [28–30].

$$\Delta\bar{\nu}(\bar{\nu}_{\text{abs}} - \bar{\nu}_{\text{em}}) = \frac{2\Delta\mu^2\Delta f}{hca^3} + \text{const} \quad (2)$$

$\Delta\nu$ is the Stokes shift, ν_{abs} and ν_{em} are wavenumbers of the absorption and fluorescence peaks, respectively. $\Delta\mu$ is the difference between the excited-state and ground-state dipole moments, h is Planck's constant, c is the

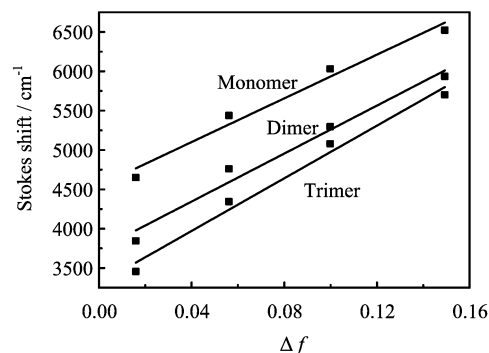


FIG. 3 Plot of Stokes shift $\Delta\nu$ versus the solvent polarity function Δf for monomer, dimer, and trimer. Solid lines are the fitted results.

velocity of light, and a is the radius of the solute spherical cavity. Δf is the solvent polarity parameter determined from the following expression:

$$\Delta f(\epsilon_r, n) = \frac{\epsilon_r - 1}{2\epsilon_r + 1} - \frac{n^2 - 1}{2(2n^2 + 1)} \quad (3)$$

where ϵ is the dielectric constant and n is the refractive index of the solvent. Plot of Stokes shift versus the solvent polarity function is shown in Fig.3. The linear relationship is obvious for all three compounds among the solvents we use. The slopes we get are nearly

TABLE II Result of Onsager radius a , ground state μ_{gr} , and excited state μ_{ex} obtained from calculation and Lippert-Mataga relationship.

	$a/\text{\AA}$	μ_{gr}/D	μ_{ex}/D	$\Delta(\mu_{\text{ex}}-\mu_{\text{gr}})/D$
Monomer	5.95	2.56	22.25	19.69
Dimer	6.00	2.76	23.40	20.63
Trimer	7.28	2.76	24.37	21.61

the same from the monomer to trimer again suggesting the similar nature of excited state and weak interaction between the branches in dimer and trimer, where the emitting state most likely arises from the relaxed ICT state localized on one branch. To qualitatively determine the polarity of the excited ICT state, we examined the dipole moment change $\Delta(\mu_{\text{ex}}-\mu_{\text{gr}})$ between the excited state and ground state dipole moments from the solvatochromic shift based on the Eq.(2). Since we have assumed that the emitting state is the same for all the chromophores independent of the branching, it would be reasonable to use Onsager radius (5.95 Å) of monomer as the effective radius of the solvent cavity for dimer and trimer to avoid the artificial overestimation of the radius of the solvent cavity [10, 12], where the Onsager cavity radii a is estimated from quantum chemical calculation by using DFT method under B3LYP/6-31G* level [10] and the ground state dipole moment is also gotten from the calculation. Table II lists the calculation results. It is found that the dipole moment in the excited-state is much larger than that in the ground state, which is consistent with the fact there is no obvious shift of the absorption spectra relative to that of the large red shifts of fluorescence spectra in various solvents, confirming our previous conclusion that excited states of the compounds enter a large degree of ICT state from the initial Franck-Condon state upon excitation. While compared with the excited state dipole moment of the three chromophores, they are almost the same, but exactly μ_{ex} is largest in trimer.

D. Fluorescence decay

To probe the population dynamic decay processes of these sample series and to address the origin of the emission state, we performed the fluorescence decay experiments by using the TCSPC technique. The obtained radiative lifetime $\tau_0=\tau/\phi$ are listed in Table III. In non-polar cyclohexane, the radiative decay time τ_0 is calculated and shows a decrease with an increase of the number of branches from 6.68 ns for monomer to 5.6 ns for trimer. A decrease in the radiative lifetime implies that the emission of the trimer may stem from delocalized excitonic states, resulting from the enhancement of the radiative rate once the exciton is formed [24, 31]. While in toluene with small polarity, the radiative lifetimes of the dimer and trimer are almost the

TABLE III Fluorescence decay time of the excited states of monomer, dimer, and trimer in solvent Cyc and Tolu.

	Cyc		Tolu	
	τ/ns	τ_0/ns	τ/ns	τ_0/ns
Monomer	3.3	6.68	4.3	7.8
Dimer	4.03	6.2	3.03	5.7
Trimer	3.7	5.6	3.08	5.7

same, but still smaller than that of the monomer. This reflects that the coupling of latter two chromophores with the solvent matrix is much weaker than that of the monomer, and the nonradiative rate shows much slower, agreeing with our calculated radiative decay rate constants k_f and nonradiative decay rate constants k_{nr} (data are not shown). All the results suggest a minor delocalization of the emitting excited states in dimer and trimer, which may be further reduced by the solvation effect [24]. Overall, the analysis about fluorescence lifetime of these sample series lead to a conclusion about the emission state that are contrary to the one obtained from steady-state absorption and fluorescence spectra. It seems that the emission of the trimer may stem from delocalized exciton states incompletely localized on one branch, where analogous phenomena has been more clearly explained in single molecule spectrum [32].

The fluorescence quantum yields of these chromophores decrease with the increasing polarity overall. On the other hand, the fluorescence yields increase with the increased chromophore branches, but from chloroform it decreases from trimer to monomer. This may result from the increased nonradiative decay rate constants k_{nr} with increased polarity [22]. Compared to the single branch molecular monomer, the dimer and trimer may have more effective coupling channels for energy dissipation, such as electronic coupling and vibronic coupling, as well as exciton splitting, which possibly enrich the TPA cross-section demonstrated by earlier researches [10, 33, 34]. These observations are complementary to our findings.

E. Femtosecond fluorescence depletion

As mentioned above, the dimer and trimer show delocalized excitation over the branches in some extent, which move to one branch very fast. Goodson had revealed the delocalization time to be less than 100 fs by time-resolved fluorescence anisotropy measurements for multibranches PRL chromophores [12, 35]. To know the detail information about the mechanism of excitation delocalization, charge localization, and nature of ICT in these series of compounds, transient measurement should be very useful. In our lab, femtosecond time-resolved fluorescence depletion technique has been proven to be a powerful method to determine the fast

TABLE IV Fitted time constants of depletion decays of monomer, dimer, and trimer in THF and Acetone.

	THF				Acetone			
	τ_1/ps	A_1	τ_2/ps	A_2	τ_1/ps	A_1	τ_2/ps	A_2
Monomer	1.03	0.79	3.60	0.21	0.91	0.96	4.92	0.04
Dimer	1.14	0.65	3.39	0.35	0.67	0.95	2.32	0.05
Trimer	0.79	0.69	3.15	0.31			1.42	

solvation processes of similar push-pull molecules in our earlier investigations [14, 15, 22], within our experimental conditions time resolution down to 200 fs has been achieved. However, predicted by both theoretical calculations and dynamic results, it is known that the ICT emitting state may delocalize some extent among the branches possessing a relatively weaker coupling with the bath in nonpolar solvent, which can be strongly affected in polar solvent [24]. This may be reasonable due to our special molecule architecture with the short vinyl groups in the middle which make electron donor and acceptor prone to achieve a planar structure for the excited states according to Ref.[10]. Goodson used the transient absorption measurements showing an increase of charge-transfer character of the excited state with an increase in branching, and this explained the relative increase in the two-photon cross section of the PRL dye series [34, 35]. As we have proved earlier if a high polarity ICT state with large dipole moment is produced upon excitation, the solvent reorganization process around the excited solute molecule will become faster [15, 18, 19, 22]. The population of such solvent stabilized ICT state is highly dependent on both solvent polarity and the polar degree of the excited ICT state, so when we employ the fluorescence depletion technique to measure the time for the solvation processes, a similar composition and time range would be expected for these compounds.

Figure 4 shows the representative femtosecond fluorescence depletion results of monomer, dimer, and trimer in solvent THF and acetone. It is found that the depletion dynamic curves of all the three compounds can be fitted well with a biexponential function in chloroform and THF. Fitting results are listed in Table IV. It is found that a fast decay with a few hundred femtosecond attributed to the vibration relaxation of the monitored emitting states and a slow decay with several picoseconds attributed to solvation dynamics related to the formation of the final relaxed ICT state, respectively [14, 15, 22]. Here, since both polarity and viscosity affect the solvation dynamic processes, we compare solvation assisted ICT dynamics of the three compounds in the same solvent. We found that both in THF and acetone, the slow decay time all decreased from monomer to trimer, which can be an indication that trimer has the largest charge-separation extent among the three studied molecules, while monomer has the smallest charge-separation extent. Thus, the fluorescence depletion measurements unambiguously show

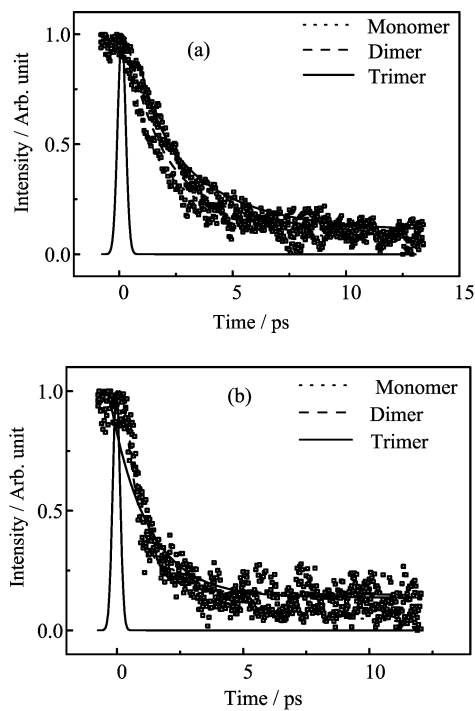


FIG. 4 Femtosecond fluorescence depletion signals of monomer, dimer and trimer in THF (a) and acetone (b). Symbols represent experimental results, and lines are fitting to experimental curves. The pump pulse is 390 nm and the probe beam is at 780 nm for all three samples. The IRF is also shown at time zero.

that the extent of charge-transfer character increases with increase in branching [12], which is very difficult to be predicted by steady-state measurements.

F. Fluorescence anisotropy

As mentioned above, the excitation in the excited state is delocated at initial time, and then locate on one arm after vibronic cooling and coupling. In order to characterize the excitation delocalization and the mechanism of energy transfer in these branched structures, we performed steady state fluorescence anisotropy measurement [22]. Figure 5 shows the anisotropy value r of the three compounds accompanied with their fluorescence excitation spectrum in polystyrene film. The values of the anisotropy r for these chromophores all reach the minimum around the 300–350 nm, which corre-

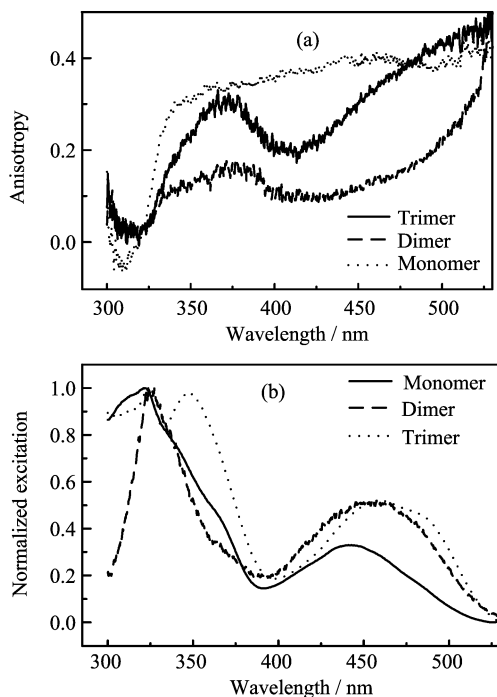


FIG. 5 (a) Fluorescence excitation anisotropy spectra and (b) normalized fluorescence excitation spectra of monomer, dimer, and trimer in an isotropic (unstretched) polystyrene film at room temperature. The excitation spectra were measured by monitoring the fluorescence all at 600 nm for monomer, dimer, and trimer.

sponds to the higher absorption band S_n . Moreover, the anisotropy of monomer keep nearly constant over the emission wavelength region 350–500 nm which means only one emission band ($S_1 \rightarrow S_0$) contributing to emission [36], and toward higher r values at longer wavelengths. While for the dimer and trimer the anisotropy values show no plateau value revealing a more complex nature of the main ICT absorption bands. Since rotational diffusion is suppressed by the dry polystyrene film, depolarization process in dimer and trimer may occur through other mechanisms, such as energy transfer or coupling between different branches. There are additional electronic transitions $S_0 \rightarrow S_n$ ($n=2, 3, \dots$) located close to $S_0 \rightarrow S_1$, or a complicated potential surface of the S_1 state may be present [37, 38]. However, in our case, excitation energy redistributed among the spatially degenerate transition dipole moments could play important role in observed anisotropic spectra [39]. The presence of intramolecular excitation transfer means that the excitation energy is randomized over the three branches of trimer during the lifetime of the excited state [10, 22]. It has been reported that the limiting r should reach 0.1 for tribranched molecule with a 3-fold symmetry if redistribution energy among the three energy-degenerate branches occurs [6]. The increase of the r could be explained by a reduction of symmetry of dimer and trimer under measurement conditions, that

the initial degenerate energy states turned to nondegenerate states when they are also coupled to the bath matrix. Our results showed that the observed r value was much higher than 0.1 [39, 40], so it is reasonable to believe that such 3-fold symmetry system in trimer breaks down along with non-degeneracy energy among the branches, and the same phenomena can be observed within dimer. When excitation occurred at the red edge of the absorption band, the branch with the least energy was the largest stabilized by solvents. Hence r increased as a result of less efficient intramolecular energy transfer between branches. On the other hand, when excitation at the high-energy side would excite the branch with a smaller solvent stabilization and hence excitation energy transfer to other branches become exergonic and more effective [39], which increase the rate of excitation transfer and decrease the anisotropy.

Furthermore, we found that the fluorescence excitation spectrum of the trimer exhibited two closely located peaks which cannot be discriminated in the absorption spectrum. One of them lies nearly the same position with the monomer at about 450 nm, which can be interpreted as the indication of the nature of excitation locating on the one arm just like the monomer, and the low-energy absorption band may be a consequence of the electric delocalization [22]. Meantime, the similar phenomenon could be seen for the dimer, but in fact, it can not be observed from the excitation spectra actually, this may also mainly due to the two exciton splitting excited state overlay the delocalization peak [10].

IV. CONCLUSION

We have examined the ICT character of the excited state as well as the dynamics of ICT states of a series of newly synthesized acceptor-donor (A- π -D) monomer, its counterpart two-branch dimer (A- π -D- π -A) and three-branch trimer (A- π)₃-D by means of steady state and femtosecond fluorescence depletion measurements. All results can provide strong evidence for the molecules of the excited-state dynamic based on both excitonic coupling delocalization and localization. The similarities of the steady-state absorption and fluorescence emission spectra, along with Lippert-Mataga relationship among the three studied compounds suggest that the excited state of the series compounds may finally locate on one branch before emission. However, the red-shift absorption, fluorescence excitation spectra and decreased experimental radiative lifetimes from the monomer to trimer show that the delocalization ICT states exist in the multi-branch compounds. Furthermore, the femtosecond fluorescence depletion measurements indicate the multibranches in fact have larger charge-separate extent relative to their single branch counterpart, and that the excitation energy is mainly redistributed between the localized ICT state with higher energy and the delocalized ICT state with much lower

energy.

V. ACKNOWLEDGMENTS

We sincerely thank Prof. Yong-fang Li for providing the samples. S. Vdović thanks CAS for support through a CAS Research Fellowship for International Young Researchers. This work was supported by National Natural Science Foundation of China, the Chinese Academy of Sciences, and the State Key Project for Fundamental Research.

- [1] J. Roncali, *Chem. Rev.* **97**, 173 (1997).
- [2] S. Roquet, A. Cravino, P. Leriche, O. Aleveque, P. Frere, and J. Roncali, *J. Am. Chem. Soc.* **128**, 3459 (2006).
- [3] G. Wu, G. Zhao, C. He, J. Zhang, Q. He, X. Chen, and Y. Li, *Sol. Energy Mater. Sol. Cells* **93**, 108 (2009).
- [4] M. Albota, D. Beljonne, J. L. Bredas, J. E. Ehrlich, J. Y. Fu, A. A. Heikal, S. E. Hess, T. Kogej, M. D. Levin, S. R. Marder, D. McCord-Maughon, J. W. Perry, H. Rockel, M. Rumi, C. Subramaniam, W. W. Webb, X. L. Wu, and C. Xu, *Science* **281**, 1653 (1998).
- [5] B. A. Reinhardt, L. L. Brott, S. J. Clarson, A. G. Dillard, J. C. Bhatt, R. Kannan, L. X. Yuan, G. S. He, and P. N. Prasad, *Chem. Mater.* **10**, 1863 (1998).
- [6] O. P. Varnavski, J. C. Ostrowski, L. Sukhomlinova, R. J. Twieg, G. C. Bazan, and T. Goodson, *J. Am. Chem. Soc.* **124**, 1736 (2002).
- [7] V. Chernyak, E. Y. Poliakov, S. Tretiak, and S. Mukamel, *J. Chem. Phys.* **111**, 4158 (1999).
- [8] J. C. Kirkwood, C. Scheurer, V. Chernyak, and S. Mukamel, *J. Chem. Phys.* **114**, 2419 (2001).
- [9] T. G. Goodson, *Acc. Chem. Res.* **38**, 99 (2005).
- [10] C. Katan, F. Terenziani, O. Mongin, M. H. V. Werts, L. Porres, T. Pons, J. Mertz, S. Tretiak, and M. Blanchard-Desce, *J. Phys. Chem. A* **109**, 3024 (2005).
- [11] G. Ramakrishna, A. Bhaskar, and T. Goodson III, *J. Phys. Chem. B* **110**, 20872 (2006).
- [12] G. Ramakrishna and T. Goodson III, *J. Phys. Chem. A* **111**, 993 (2007).
- [13] J. N. Demas, and G. A. Crosby, *J. Phys. Chem.* **75**, 991 (1971).
- [14] X. Guo, S. Wang, A. Xia, and H. Su, *J. Phys. Chem. A* **111**, 5800 (2007).
- [15] Y. Gong, X. Guo, S. Wang, H. Su, A. Xia, Q. He, and F. Bai, *J. Phys. Chem. A* **111**, 5806 (2007).
- [16] Q. H. Zhong, Z. H. Wang, Y. Sun, Q. H. Zhu, and F. N. Kong, *Chem. Phys. Lett.* **248**, 277 (1996).
- [17] Y. He, Y. J. Xiong, Z. H. Wang, Q. H. Zhu, and F. N. Kong, *J. Phys. Chem. A* **102**, 4266 (1998).
- [18] J. Y. Liu, W. H. Fan, K. L. Han, W. Q. Deng, D. L. Xu, and N. Q. Lou, *J. Phys. Chem. A* **107**, 10857 (2003).
- [19] J. Y. Liu, W. H. Fan, K. L. Han, D. L. Xu, and N. Q. Lou, *J. Phys. Chem. A* **107**, 1914 (2003).
- [20] J. L. Bredas, D. Beljonne, V. Coropceanu, and J. Cornil, *Chem. Rev.* **104**, 4971 (2004).
- [21] J. S. Yang, J. L. Yan, C. Y. Hwang, Y. Shih, Chiou, K. L. Liau, H. H. G. Tsai, G. H. Lee, and S. M. Peng, *J. Am. Chem. Soc.* **128**, 14109 (2006).
- [22] M. Jia, X. Ma, L. Yan, H. Wang, Q. Guo, X. Wang, Y. Wang, X. Zhan, and A. Xia, *J. Phys. Chem. A* **114**, 7345 (2010).
- [23] W. Verbouwe, L. Viaene, M. VanderAuweraer, F. C. DeSchryver, H. Masuhara, R. Pansu, and J. Faure, *J. Phys. Chem. A* **101**, 8157 (1997).
- [24] Y. Wang, G. S. He, P. N. Prasad, and T. Goodson, *J. Am. Chem. Soc.* **127**, 10128 (2005).
- [25] A. J. Wise, T. P. Martin, J. Gao, K. VanDerGeest, and J. K. Grey, *J. Chem. Phys.* **133**, 174901 (2010).
- [26] T. Liu, J. S. Gao, B. H. Xia, X. Zhou, and H. X. Zhang, *Polymer* **48**, 502 (2007).
- [27] M. L. Horng, J. A. Gardecki, A. Papazyan, and M. Maroncelli, *J. Phys. Chem.* **99**, 17311 (1995).
- [28] N. Mataga, Y. Kaifu, and M. Koizumi, *Bull. Chem. Soc. Jpn.* **29**, 465 (1956).
- [29] E. Lippert, *Zeitschrift Fur Elektrochemie* **61**, 962 (1957).
- [30] N. Mataga, *Bull. Chem. Soc. Jpn.* **36**, 654 (1963).
- [31] J. Grad, G. Hernandez, and S. Mukamel, *Phys. Rev. A* **37**, 3835 (1988).
- [32] D. Aumiler, S. Wang, X. Chen, and A. Xia, *J. Am. Chem. Soc.* **131**, 5742 (2009).
- [33] D. Beljonne, W. Wenseleers, E. Zojer, Z. G. Shuai, H. Vogel, S. J. K. Pond, J. W. Perry, S. R. Marder, and J. L. Bredas, *Adv. Funct. Mater.* **12**, 631 (2002).
- [34] P. Macak, Y. Luo, P. Norman, and H. Agren, *J. Chem. Phys.* **113**, 7055 (2000).
- [35] S. J. Chung, K. S. Kim, T. H. Lin, G. S. He, J. Swiatkiewicz, and P. N. Prasad, *J. Phys. Chem. B* **103**, 10741 (1999).
- [36] J. R. Lakowicz, *Principles of Fluorescence spectroscopy*, 2nd Ed New York: Kluwer Academic/Plenum Publishers (1999).
- [37] F. Terenziani, A. Painelli, C. Katan, M. Charlot, and M. Blanchard-Desce, *J. Am. Chem. Soc.* **128**, 15742 (2006).
- [38] A. R. Morales, K. J. Schafer-Hales, C. O. Yanez, M. V. Bondar, O. V. Przhonska, A. I. Marcus, and K. D. Belfield, *ChemPhysChem* **10**, 2073 (2009).
- [39] W. Verbouwe, M. Van der Auweraer, F. C. De Schryver, J. J. Piet, and J. M. Warman, *J. Am. Chem. Soc.* **120**, 1319 (1998).
- [40] R. D. Hall, B. Valeur, and G. Weber, *Chem. Phys. Lett.* **116**, 202 (1985).